

Distinctive Features of the Structure of Current Sheets Formed in Plasma in Three-Dimensional Magnetic Configurations with an X line (a Review)

A. G. Frank*

Prokhorov General Physics Institute of the Russian Academy of Sciences, Moscow, 119991 Russia

**e-mail: annfrank@fpl.gpi.ru*

Received November 25, 2021; revised November 25, 2021; accepted November 25, 2021

Abstract—A review is presented of experimental results of the studies of the distinctive features of the structure and evolution of plasma current sheets that are formed in three-dimensional (3D) magnetic configurations with an X line in the presence of a longitudinal magnetic field component (guide field) directed along the X line. It is shown that, during the development of the current sheet, the longitudinal component of the guide field increases within the sheet. The excess guide field is sustained by the plasma currents that flow in the transverse plane with respect to the main current in the sheet, and as a result, the current structure becomes three-dimensional. When the guide field increases, the degree of compression into the sheet decreases, both of the electric current and the plasma, which is caused by the change in the balance of pressures in the sheet with the appearance of excess guide field. The deformation of plasma current sheets, and in particular, the appearance of asymmetrical and tilted current sheets in 3D magnetic configurations results from the excitation of Hall currents and their interaction with the guide field. It is shown that the formation of current sheets in 3D magnetic configurations with an X line is possible in a relatively wide but limited range of initial conditions.

Keywords: plasma, current sheet, magnetic reconnection, three-dimensional magnetic configurations, X line, Hall currents

DOI: 10.1134/S1063780X22200144

1. INTRODUCTION

The processes of magnetic reconnection and the transformation of magnetic energy into the energy of the plasma and the accelerated particles occur in the regions of magnetized plasma where magnetic field lines of opposite (or different) directions approach each other. These regions are characterized by high densities of electric current and small sizes, so even under condition of high plasma conductivity, the effect of dissipation processes becomes substantial. In these regions, the condition of magnetic field being frozen in matter is violated, which leads to the reconnection of oppositely directed magnetic field lines and transformation of magnetic energy into thermal and kinetic energy of the plasma and the energy of accelerated particles and radiation. The regions of the plasma in which the electric current is concentrated and which separate magnetic fields of the opposite directions usually take the shape of current sheets [1–4].

Under real conditions, i.e., in space objects and installations for confinement and heating of the plasma, the magnetic fields are usually three-dimensional (3D). Therefore, the study of the possibility of

formation of current sheets in 3D magnetic configurations and the analysis of the distinctive features of current sheets that can be formed in such configurations is of a principle importance for the problem of magnetic reconnection as a whole.

Among the wide variety of 3D magnetic configurations, of special interest are configurations that contain X lines due to their roles in the formation of current sheets and, consequently, in magnetic reconnection phenomena [1]. In 3D configurations with X line, the magnetic field can not turn zero anywhere, and at the same time, both transverse components of the magnetic field are zero at the X line, similar to configurations with a null line. Along the X line, longitudinal magnetic field can be present, which distinguishes the X line from its particular case, the null line. In general, the magnetic configuration with X line is a more general configuration than the configurations that contain both null lines and null points. In configurations with isolated null points, the X line is present both in the region of null magnetic field and away from this region.

The simplest magnetic configuration with X line can be written as

$$\mathbf{B}(x, y) = \{B_x; B_y; B_z\} = \{h \times y; h \times x; B_z^0\}. \quad (1)$$

Here, \mathbf{B} is the vector of magnetic field induction, B_x , B_y , and B_z are its components in the Cartesian coordinates system, (x, y) are the coordinates of an arbitrary point in which the vector \mathbf{B} is determined, the X line follows the Oz axis; along the same axis the uniform longitudinal field component B_z^0 is directed, and the magnetic field in the (x, y) plane is characterized by the constant gradient h . Magnetic field \mathbf{B} does not become zero anywhere, and neither of its components depends on coordinate z .

Note also that the magnetic configuration (1) has a number of advantages for experimental studies, in particular, from the diagnostic viewpoint. It allows one to efficiently apply interferometric methods that measure parameters averaged over the line of sight (see below).

It was shown in a number of experiments that the formation of current sheets can occur in 3D configurations in the presence of a relatively strong longitudinal magnetic field component directed along the X line [5–10]. The current sheet has two substantially different sizes in the transverse (relative to the X line) plane (x, y) : the width of the sheet (in this case, its size in the x direction) usually exceeds the thickness (its size along the y axis) approximately by an order of magnitude. In this, the current sheets formed in 3D configurations are quite close to the sheets that develop in the 2D magnetic configurations with null line [11, 12].

At the same time, the current sheets that develop in 3D magnetic configurations can substantially differ from current sheets in 2D configurations by a number of parameters. These differences can affect the processes of magnetic reconnection and, consequently, the processes of transformation of magnetic energy into the thermal and kinetic energy of the plasma and the energy of accelerated particles and radiation.

In this review, we generalize and organize the earlier obtained experimental data on the plasma parameters and structural features of current sheets that were formed in 3D magnetic configurations with X line (1) at different ratios between the transverse magnetic field gradient h and the longitudinal field component B_z^0 . Our main focus of attention here is the effect of the longitudinal magnetic field component on the characteristics of current sheets. The experimental results presented in this work were obtained in the plasma of the CS-3D device (Prokhorov General Physics Institute of the Russian Academy of Sciences) using different diagnostic methods.

2. EXPERIMENTAL DEVICE AND DIAGNOSTIC METHODS

3D magnetic configurations (1) are produced in the CS-3D device (Fig. 1) by superposition of two magnetic fields: the 2D field with a null line of X type along the Oz axis and the gradient $h \leq 1$ kG/cm, and the uniform longitudinal field with induction $B_z^0 \leq 8$ kG [5, 6, 12]. Each field is induced independently, which allows us to form magnetic configurations with different ratios between h and B_z^0 . Both magnetic fields are quasi stationary relative to the faster plasma processes.

The quartz vacuum chamber with diameter $2R_C = 18$ cm and length 100 cm is initially evacuated and then filled with one of the noble gases: argon (Ar), krypton (Kr), or helium (He). The initial plasma with electron density $N_e^0 \approx 10^{14} - 5 \times 10^{15} \text{ cm}^{-3}$ and ionization degree 40–70% is produced in magnetic field (1) by ionization of the neutral gas with the Θ discharge with a strong initial preionization. Then, the electric current J_z directed parallel to the X line of magnetic field (1) is induced in the plasma. The half-period of the current is $T/2 = 6 \mu\text{s}$ and its amplitude is $J_z^0 \approx 46 - 50$ kA. The plasma current J_z initiates plasma flows in the (x, y) plane, which then lead to the formation of the current sheet, i.e., to current concentrating in the vicinity of the plane $(y = 0)$ (at certain directions of field (1) and current J_z), see Fig. 1.

For diagnostics, in our experiments we used magnetic measurements [13–17], holographic interferometry [8, 10, 18–21], and spectroscopic methods [22–24].

The structure of the magnetic field was studied using a set of magnetic probes that were moved either along the surface of the sheet (line AA' , $y = 0.8$ cm) or across the sheet, at two distances from the X line (BB' , $x = -0.8$ cm and CC' , $x = -5$ cm), Fig. 1b. In each point, the probes registered time variations of the three mutually perpendicular components of the magnetic field created by the plasma currents. Based on these measurements, the space–time characteristics of the magnetic fields and electric currents were determined. The 2D distributions of electron concentration N_e in the (x, y) plane were recorded by holographic interferometry. The thermal and directed velocities of ions, the electron temperature, and the plasma concentration were determined using spectral measurements.

3. FORMATION OF THE CURRENT SHEET IN THE MAGNETIC FIELD WITH X LINE AND AMPLIFICATION OF THE LONGITUDINAL COMPONENT OF THE MAGNETIC FIELD IN THE SHEET

The formation of a current sheet in 3D magnetic configurations with X line starts from the propagation

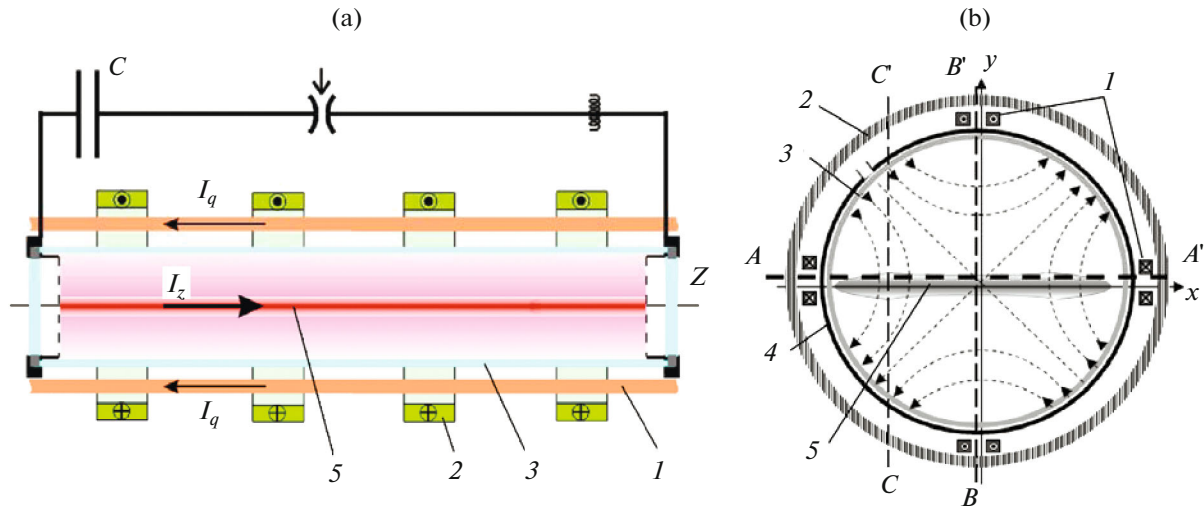


Fig. 1. Scheme of the CS-3D device: (a) side view and (b) cross section. 1—Current conductors used to excite the 2D (transverse) magnetic field whose lines are shown in panel (b) by dashed lines with arrows; 2—current coils used to excite the longitudinal field B_z^0 ; 3—vacuum chamber; 4—coils of the Θ discharge used to generate the initial plasma; and 5—plasma current sheet. AA' , BB' , and CC' in panel (b) are lines along which magnetic probes were moved.

of a magnetosound wave in plasma [15]. The excitation of plasma current J_z directed in parallel to the X line initiates perturbations of the transverse magnetic field in the (x, y) plane near the side boundaries of the plasma, similarly to the same process in the 2D configuration with a null line [25].

This is seen in Fig. 2a, where perturbations of the tangential component of magnetic field $\delta B_x(y)$ are shown at consecutive times. Perturbations δB_x appear near the plasma boundaries (Fig. 2a, $t \cong 0.5; 1.0 \mu\text{s}$) and propagate from the both sides in the direction of the X line located at $y = 0$. As the wave front approaches the X line, the values of δB_x and derivatives $\partial B_x / \partial y$, i.e., the current density j_z , increase, see Fig. 2a, $t \cong 1.5; 2.0 \mu\text{s}$.

The propagation of the magnetosound wave in plasma in magnetic field (1) at $B_z^0 \neq 0$ is also accompanied by the appearance of perturbations of the longitudinal field component δB_z (fig. 2b, $t \cong 1.0 \mu\text{s}$). From comparison of the curves in Figs. 2a and 2b that correspond to the same time, it is seen that perturbations δB_x and δB_z appear simultaneously in the same regions of space. A substantial increase in δB_z occurs when the wave front approaches the X line, Fig. 2b, $t \cong 1.5 \mu\text{s}$.

At $t \cong 2.0 \mu\text{s}$, when the magnetosound wave reaches the X line (Fig. 2a), the density of plasma current j_z increases sharply, and the size of the region of current localization along the y axis decreases: the current is compressed in the y direction, i.e., the formation of the current sheet takes place. At the same time, as is seen from Fig. 2b, in the midplane of the current

sheet, at $y \cong 0$, δB_z increases substantially and reaches its maximum value, $\delta B_z \cong 0.9 \text{ kG}$, by the time $t \cong 3.0 \mu\text{s}$, while the halfwidth of the distribution $\delta B_z(y)$ is $2\delta y \cong 1.2 \text{ cm}$.

Note that the direction of the additional longitudinal field δB_z in the plasma current sheet always coincides with the direction of the magnetic field component B_z^0 of the initial magnetic configuration (1).

This is seen from comparison of curves 1 and 2 in Fig. 3, which characterize the change of δB_z during the formation of current sheets in two magnetic configurations (1) with oppositely directed B_z^0 . From this, it follows that during the formation of the current sheet in the magnetic configuration with X line, the longitudinal component of the magnetic field increases compared to its initial value B_z^0 [15].

Note also that the increase of the longitudinal component occurs over the entire width of the current sheet, both in the vicinity of the X line, at $x = -0.8 \text{ cm}$ (Fig. 3a) and at a substantial distance from the X line, at $x = -5 \text{ cm}$ (Fig. 3b).

Thus, the flows of plasma that appear in the (x, y) plane and result in the formation of the current sheet also carry into the vicinity of the X line the longitudinal component of the magnetic field, which leads to it increase within the current sheet. This effect demonstrates that the magnetic field is frozen into the plasma.

The additional longitudinal field δB_z is present in those and only those regions of the current sheet, where the main current j_z is concentrated. The distri-

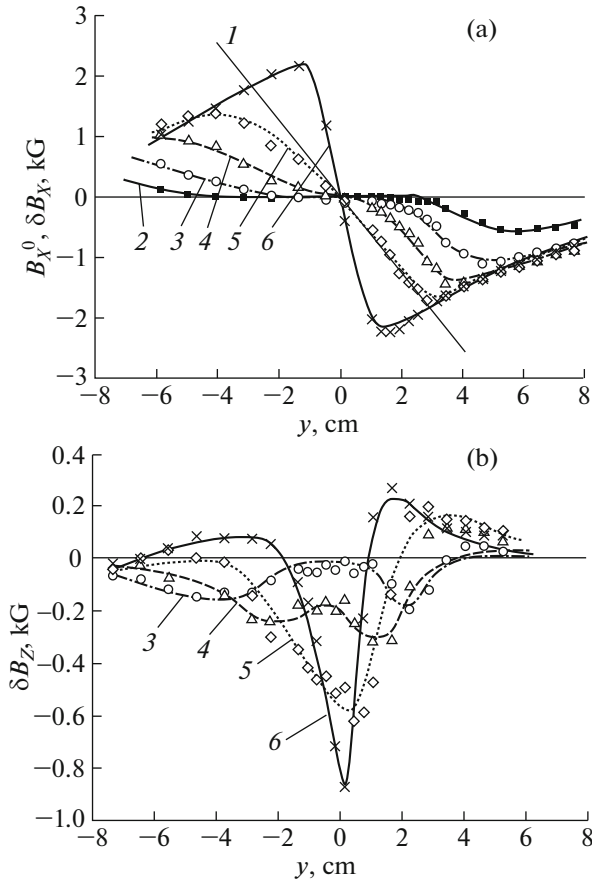


Fig. 2. Propagation of perturbations of (a) the tangential magnetic field component $\delta B_X(y)$ and (b) the longitudinal component $\delta B_Z(y)$ along line BB' ($x = -0.8 \text{ cm}$) in the current sheet plasma at consecutive times: (1) $B_Z^0 = hy$ is the tangential component of the vacuum magnetic field; $t =$ (2) 0.5, (3) 1.0, (4) 1.5, (5) 2.0, and (6) 3.0 μs . Experimental conditions: $B_Z^0 = -2.9 \text{ kG}$, $h = 0.64 \text{ kG/cm}$, Kr, $p = 36 \text{ mTorr}$, and $J_Z^{\text{max}} = 48 \text{ kA}$.

bution of current $j_Z(y)$ and in particular, the transverse width of the sheet $2\Delta y$ can change both with time and when the initial longitudinal magnetic field B_Z^0 is changed. At this, the distributions $\delta B_Z(y)$ at every time and at different fields B_Z^0 almost completely repeat the current distributions $j_Z(y)$ [15]. Thus, during the evolution of the current sheet, the width of the sheet $2\Delta y$ decreases, i.e., the plasma current is concentrated in the region near $y = 0$, and at the same time, the region of increased field δB_Z also decreases. Comparison of Figs. 4a and 4b shows that the formation of the sheet at high values of longitudinal component B_Z^0 leads both to the increase of the sheet width $2\Delta y$ and the size of the region of increased field δB_Z (see also [8, 10, 13, 18]).

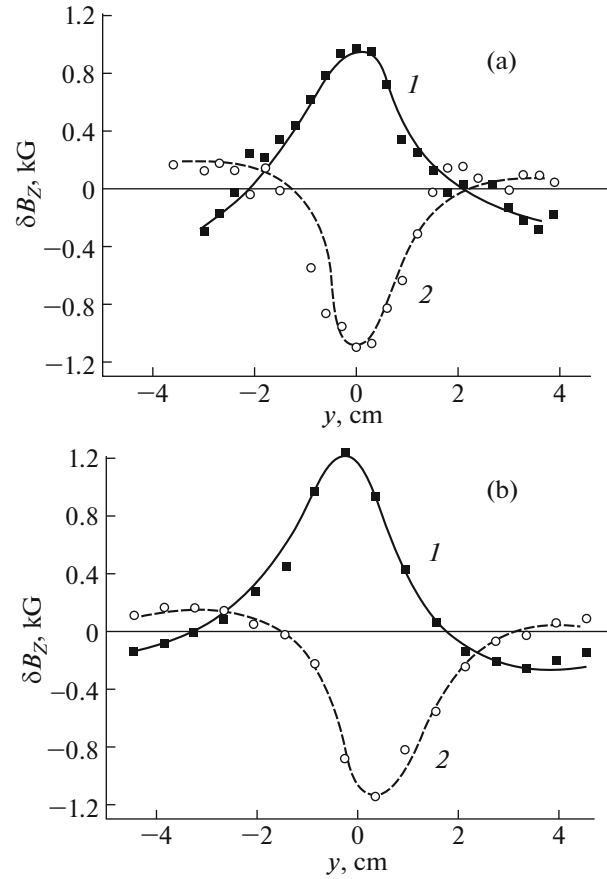


Fig. 3. Distributions of longitudinal magnetic field perturbations $\delta B_Z(y)$ in the plasma current sheet at two opposite directions of initial field B_Z^0 . Measurements were carried out along two lines: (a) BB' ($x = -0.8 \text{ cm}$) and (b) CC' ($x = -5 \text{ cm}$). Curves 1 were obtained at $B_Z^0 = +2.9 \text{ kG}$; curves 2 at $B_Z^0 = -2.9 \text{ kG}$. Experimental conditions: $h = 0.57 \text{ kG/cm}$, Kr, $p = 36 \text{ mTorr}$, $t = 3 \mu\text{s}$, and $J_Z^{\text{max}} = 50 \text{ kA}$.

4. ELECTRIC CURRENTS IN THE TRANSVERSE PLANE (x, y) THAT PROVIDE THE AMPLIFICATION OF THE LONGITUDINAL COMPONENT IN THE PLASMA CURRENT SHEET

From general physical considerations, it is clear that the excess magnetic field δB_Z in the current sheet that forms in a 3D magnetic configuration with X line can exist only due to electric currents in the transverse plane with respect to the X line and the main current in the sheet J_Z .

Based on results of measurements of space distributions of δB_Z , it is possible to estimate the current density in the (x, y) plane taking into account that both the magnetic field and the plasma are uniform in the z direction ($\partial/\partial z \cong 0$). Since in current sheet, usually $\partial B_Z/\partial y \gg \partial B_Z/\partial x$, then the electric current that

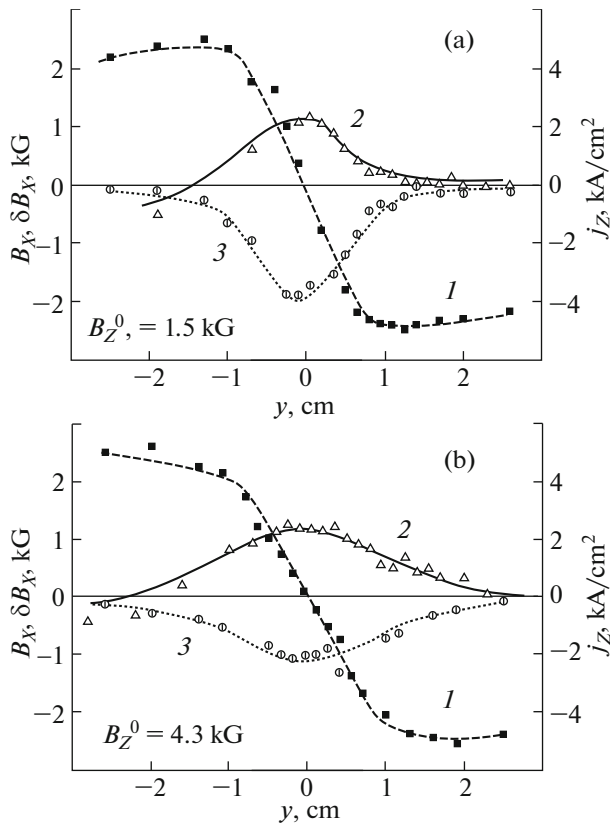


Fig. 4. Distributions along line BB' ($x = -0.8$ cm) of (1) tangential magnetic field component of the current sheet B_X , (2) perturbation of longitudinal component δB_Z , and (3) current density in the current sheet j_Z at two values of the initial longitudinal field: $B_Z^0 =$ (a) 1.5 kG and (b) 4.3 kG. Experimental conditions: $h = 0.5$ kG/cm, Ar, $p = 28$ mTorr, and $J_Z^{\max} = 50$ kA.

ensures the existence of the increased longitudinal magnetic field is mainly the current j_X that flows along the surface of the sheet:

$$j_X(y) = c/4\pi\partial B_Z/\partial y. \tag{2}$$

Figures 5a and 5b show distributions of current $j_X(y)$ together with distributions of the main (longitudinal) current $j_Z(y)$ in two cross sections: $x = -0.8$ cm and $x = -5$ cm [26]. Distributions $j_Z(y)$ have the shape of bell-like curves with currents of one direction that is independent of the direction of the longitudinal magnetic field component B_Z^0 . Transverse currents $j_X(y)$ are localized in the same areas as currents $j_Z(y)$, but they are directed oppositely at $y < 0$ and $y > 0$, while the reversal of the direction of current j_X occurs in the region where the main current j_Z is maximum. Note also the obvious fact that the directions of currents j_X also reverse when the direction of field B_Z^0 is reversed and, consequently, when the direction of the longitu-

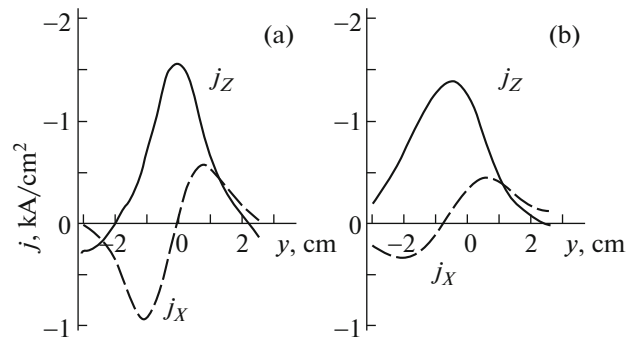


Fig. 5. Distributions along the y axis of the main (longitudinal) current $j_Z(y)$ and transverse currents $j_X(y)$: $x =$ (a) -0.8 cm and (b) -5 cm. Experimental conditions: $B_Z^0 = +2.9$ kG, $h = 0.5$ kG/cm, Ar, $p = 28$ mTorr, $J_Z^0 \approx 46$ kA, and $t = 2.2$ μ s.

dinal component that is increased within the sheet is reversed [15, 26].

It follows that as a result of the increase of the longitudinal component and the appearance of transverse currents j_X , the complexity of the structure of currents in the sheet increases substantially, since at different regions shifted along the normal to the midplane of the current sheet the total currents are not parallel, but inclined with respect to one another. The current structure is shown in Fig. 6, where the distribution of total currents is shown depending on the y coordinate [26]. The total currents are shown as vectors whose ends are connected by the solid line; the longitudinal currents $j_Z(y)$ are the black vertical lines in plane (y, j_Z) ; and the transverse currents $j_X(y)$ are the dashed curves in plane (j_X, y) . In other words, the current distribution in the sheet differs substantially from the planar “ribbon” current. Thus, during the formation of the current sheet in the magnetic configuration with X line, the structure of both magnetic fields and currents becomes three-dimensional.

5. DISTINCTIVE FEATURES OF THE COMPRESSION OF ELECTRIC CURRENT AND PLASMA INTO A CURRENT SHEET IN MAGNETIC FIELDS WITH X LINE

Comparison of current sheets that developed in magnetic configurations with X line at different values of longitudinal component B_Z^0 or in its absence shows substantial differences in distributions of main current j_Z and of plasma density in the sheet. One of the main effects is the decreasing efficiency of compression of the electric current and plasma into the sheet with increasing longitudinal component B_Z^0 .

It is seen in Figs. 7a and 7b that when B_Z^0 is increased from 0 to 4.35 kG, the width of the current

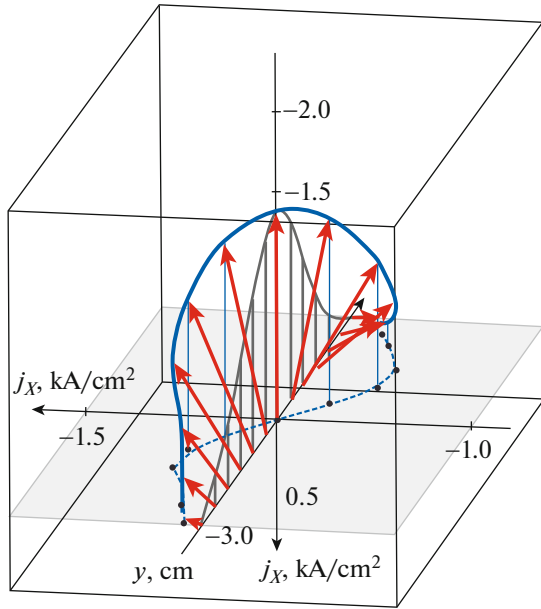


Fig. 6. Structure of total currents j_S in coordinates j_X, y, j_Z at $x = -5$ cm. The experimental conditions are the same as in Fig. 5.

sheet $2\Delta y$ increased from 1.2 to 2.9 cm, while at the same time, the current density j_Z^{\max} in the midplane of the sheet decreased from 3.75 to 2.1 kA/cm² [13]. This effect is also seen in Fig. 4, since the width of the cur-

rent sheet at $B_Z^0 = 4.3$ kG (Fig. 4b) substantially exceeds its width at $B_Z^0 = 1.5$ kG (Fig. 4a).

Similar dependences were found when studying the plasma compression into the current sheet in magnetic configurations with X line [6, 8, 10, 18]. When current sheets develop in 2D magnetic fields with null line (the longitudinal component $B_Z^0 = 0$), an effective compression of plasma into the sheet occurs, so that the maximum concentration of electrons in the midplane of the sheet can more than 10 times exceed the density of the plasma that surrounds the sheet and the density of initial plasma [11, 27–29]. However, in 3D configurations with X line in the presence of longitudinal magnetic field component B_Z^0 , the plasma density in the sheet decreases, which was first recorded based on spectral measurements [6].

The specific features of compression into the sheet of the plasma that was created by ionizing different neutral gases were studied in detail by holographic interferometry [8, 10, 18, 21]. In these works, the main attention was paid to studying the structure of the current sheet depending on magnetic field topology. Interferograms of the plasma of current sheets were recorded that developed under different conditions, and based on those, 2D distributions of electron concentration $N_e(x, y)$ were obtained. Here, we will consider the effect of the longitudinal magnetic field component on the most important parameters of plasma current sheets.

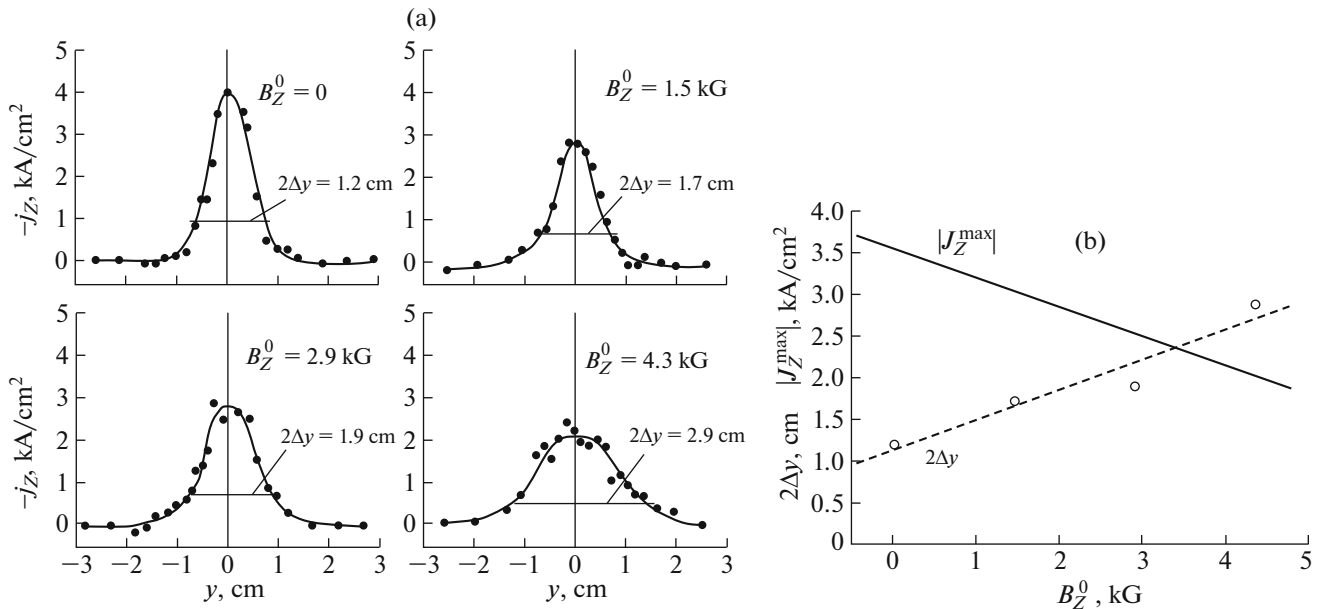


Fig. 7. (a) Distributions of current density $j_Z(y)$ over the plasma current sheet width at $B_Z^0 = 0; 1.5; 2.9; 4.3$ kG and (b) experimental dependence of current density and sheet width $2\Delta y$ at the level $0.25 j_Z^{\max}$ on the field B_Z^0 . Experimental conditions: $h = 0.5$ kG/cm, Ar, $p = 28$ mTorr.

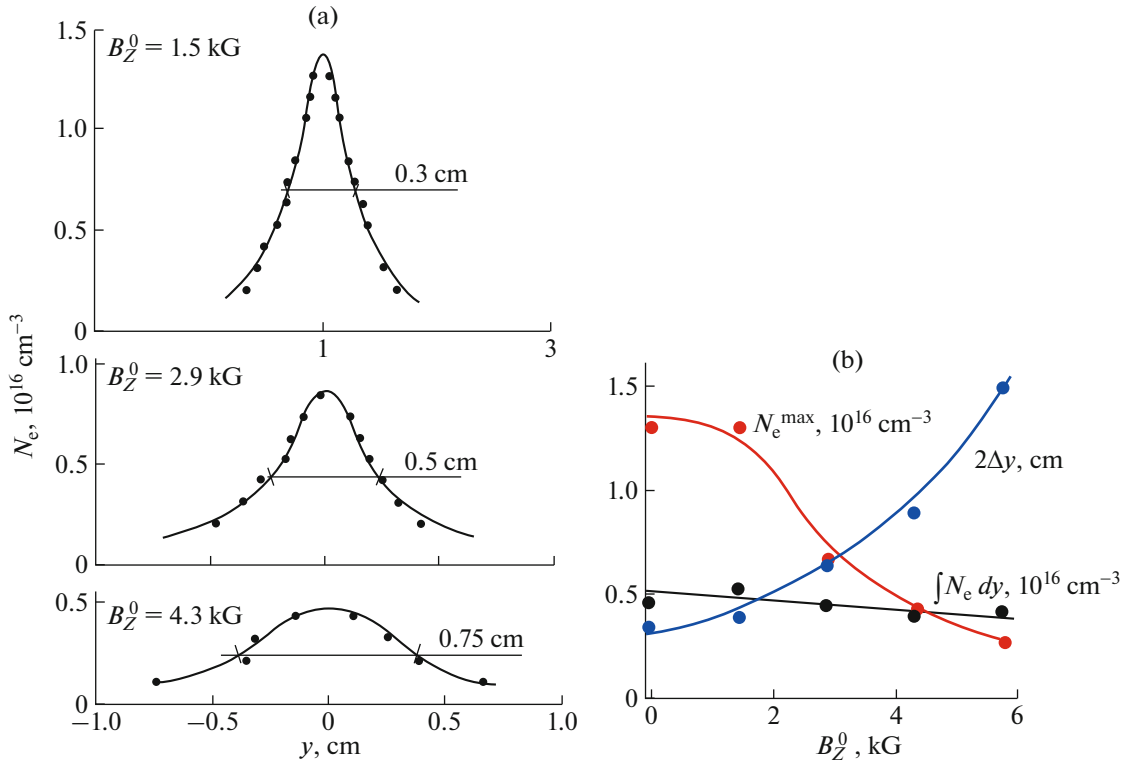


Fig. 8. (a) Electron concentration $N_e(y)$ profiles in the central region ($x \approx 0$) of the current sheet formed in 3D magnetic field with X line at $B_Z^0 = 1.5; 2.9; 4.3$ kG and (b) dependences on B_Z^0 of the maximum electron concentration N_e^{\max} in the midplane of the sheet, the sheet thickness $2\Delta y$ at the level $0.5N_e^{\max}$, and the integral over the sheet thickness of number of electrons per 1 cm of sheet width. Experimental conditions: $h = 0.43$ kG/cm, $J_Z^{\max} \approx 50$ kA, Ar, $p = 28$ mTorr, and $t \approx 3 \mu\text{s}$.

The distributions of plasma concentration $N_e(y)$ over the sheet width in its central region ($x \cong 0$) shown in Fig. 8a for three values of B_Z^0 show clearly that the triple increase in B_Z^0 leads to a decrease in the maximum electron concentration in the midplane of the sheet $N_e^{\max} \approx 3$ times and a simultaneous increase in the sheet width ≈ 2.5 times.

The dependences of the parameters of the plasma sheet formed in Ar on the longitudinal component B_Z^0 are shown in Fig. 8b. These are N_e^{\max} , the sheet width $2\Delta y_{1/2}$ at the level $0.5 \times N_e^{\max}$, and the total number of electrons per 1 cm of sheet width integrated over the sheet thickness, $N_e^{\text{tot}} = \int N_e(y) dy \approx N_e^{\max} \times 2\Delta y_{1/2}$. This data relate to the central region of the sheet ($x \cong 0$) and correspond to time $t \cong 3 \mu\text{s}$. It is seen in Fig. 8b that both maximum electron concentration N_e^{\max} and sheet width $2\Delta y_{1/2}$ are very sensitive to the value of the longitudinal component B_Z^0 , whose increase leads to the decrease in N_e^{\max} and increase in the sheet width. When B_Z^0 changes from 0 to 5.8 kG, the maximum

electron concentration decreases from 1.3×10^{16} to $0.26 \times 10^{16} \text{ cm}^{-3}$ while simultaneously, the sheet width increases from 0.35 to 1.4 cm. It is seen that as a result, the gradient of plasma density decreases in the direction perpendicular to the sheet surface. Note that the total number of electrons per 1 cm of the sheet width is almost independent of B_Z^0 (with an accuracy of about 20%).

The dependences shown here demonstrate that the presence of the longitudinal magnetic field component in the 3D magnetic configuration with X line leads to the decrease of the degree of electric current and plasma compression into the sheet.

It is natural to connect the decrease of the efficiency of current and plasma compression with the increase of the longitudinal magnetic field component in the sheet compared to its value outside the sheet (see above).

The presence of additional longitudinal field δB_Z in the sheet changes the condition of transverse equilibrium of the plasma concentrated in the sheet. In this case, the equilibrium condition should be written as

$$8\pi \times N_e^{\max} \times (T_e + T_i/Z_i) + (\delta B_Z)^2 = (B_X^{\text{sh}})^2. \quad (3)$$

Here, T_e and T_i are the electron and ion temperatures in the midplane of the current sheet, respectively, Z_i is the effective ion charge, δB_z is the excess longitudinal component in the sheet compared to the value outside of it, and B_x^{sh} is the tangential magnetic field component near the surface of the sheet. From Eq. (3), it is seen that excess longitudinal magnetic field δB_z creates excess magnetic pressure $(\delta B_z)^2/8\pi$ inside the sheet, which, together with gas kinetic pressure $N_e^{max}(T_e + T_i/Z_i)$ should be balanced by the magnetic field pressure outside the sheet $(B_x^{sh})^2/8\pi$. Thus, the appearance of excess magnetic field δB_z in the current sheet should lead (all other conditions being equal) to a decrease in the maximum electron concentration N_e^{max} .

6. DEFORMATION OF PLASMA CURRENT SHEETS FORMED IN 3D CONFIGURATIONS WITH X LINE AND THE LONGITUDINAL MAGNETIC FIELD COMPONENT UNDER GENERATION OF HALL CURRENTS IN THE SHEET

Another interesting effect was discovered in current sheets that develop in 3D magnetic configurations with X line. In the presence of longitudinal magnetic field component B_z^0 directed along the X line, the peripheral (side) regions of current sheet experience oppositely directed deviations from its midplane ($y = 0$) so that the sheet becomes tilted and asymmetric [19–21]. Such deviations manifest in the space distributions of current flowing in the sheet and plasma concentrated in the sheet. The deviations are maximum at the early stage of sheet evolution and decrease with time, while the sign of the deviation reverses when the direction of the longitudinal magnetic field component B_z^0 is reversed. This effect is completely absent in current sheets that develop in 2D magnetic configurations with null line.

Figure 9 shows 2D distributions of electron concentration $N_e(x, y)$ in three current sheets that were formed in 3D magnetic fields with X line at different values of the longitudinal magnetic field component: $B_z^0 = -2.9; 0; +2.9$ kG with all other experimental conditions being equal. If at $B_z^0 = 0$, a flat and symmetrical sheet appears that is located near the plane $y = 0$, then in the presence of longitudinal component $B_z^0 = \pm 2.9$ kG, the side ends of the sheet deviate from its midplane. The reversal of the B_z^0 direction causes the reversal of asymmetry, i.e., the direction of deviation of the ends of the sheet and reorientation of the sheet, Fig. 9.

Note that the asymmetry of the sheets and the deviation of their ends from the midplane are maximum at

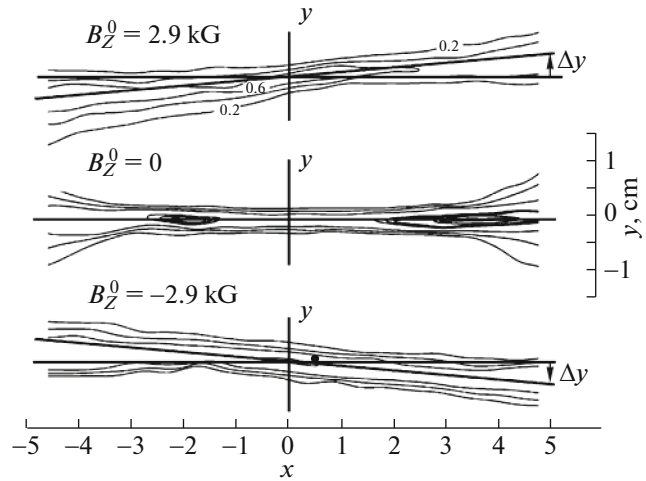


Fig. 9. Structure of plasma of current sheets shown by lines of equal plasma density. The change of density between neighboring lines is $2 \times 10^{15} \text{ cm}^{-3}$. The current sheets were formed in magnetic configurations (1) at different directions of the longitudinal magnetic field component: B_z^0 : +2.9 kG; 0; -2.9 kG. Experimental conditions: $h = 0.57 \text{ kG/cm}$, $J_z^{max} \approx 50 \text{ kA}$, Kr, $p = 36 \text{ mTorr}$, and $t \approx 3 \mu\text{s}$.

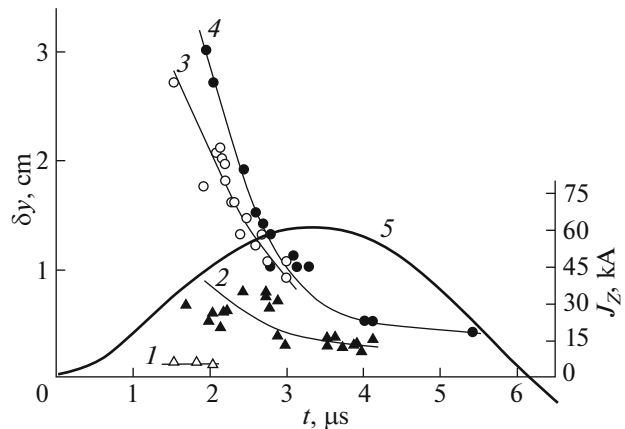


Fig. 10. Time dependences of deviations of plasma sheets δy from the midplane ($y = 0$) at $x = -5 \text{ cm}$. The current sheets were formed in different gases: 1—He, 2—Ar, 3—Kr, and 4—Xe; 5— $J_z(t)$. Experimental conditions: $h = 0.57 \text{ kG/cm}$, $B_z^0 \approx +2.9 \text{ kG}$.

the early stage of sheet evolution and decrease with time. When current sheets were formed in plasma with ions of different mass, it was found that both the deviation of the sheet ends and the time interval during which these deviations exist increase with increasing mass of plasma ions, Fig. 10.

The presented experimental data and the analysis of the plasma parameters allow us to draw the conclusion that the deformations of current sheets in 3D magnetic configurations are caused by the exci-

tation of Hall currents and appearance of additional dynamic effects during the interaction of Hall currents with the longitudinal magnetic field component [12, 17, 19, 20].

It is known that generation of Hall currents is caused by the motion of electrons relative to the inertial and slow-moving ions. The acceleration of ions along the sheet surface, from its midplane to the ends, leads to a gradual decay of Hall currents, and when the mass of plasma ions is increased, the characteristic time during which Hall currents are flowing increases [14]. While the Hall currents are decaying, the electrodynamic forces that cause the deformation of the current sheet decrease, and as a result, the deviation of the peripheral regions of the sheet from its midplane also decreases.

In current sheets formed in 2D configurations with null line, Hall currents are also excited. They were recorded and analyzed in [14, 26, 30–33]. However, in the absence of longitudinal component B_Z^0 , no additional forces appear that are capable of deforming the sheet, and in this case, the current sheet remains flat and symmetric.

Studies of the evolution of current density distribution over the sheet width $j_z(y)$ in the peripheral region of the sheet ($x = -5$ cm) showed that in the presence of the longitudinal magnetic field component, the maximums of current profiles j_z^{\max} shift relative to the plane $y = 0$ [17]. Figure 11 shows the time dependences of these shifts for three values of B_Z^0 , wherefrom it follows that when the direction of B_Z^0 is reversed, the maximum of the current profile j_z^{\max} also shifts in the opposite direction. The values of deviations j_z^{\max} agree satisfactorily with the deviations of the maximums of plasma density, i.e., there is a correlation between the distributions of current density and plasma density in asymmetric current sheets.

It is seen from Fig. 11 that at the late stage of evolution of the current sheet, the deviations of its peripheral regions can abruptly change direction relative to the plane $y = 0$. If at the initial stage ($t = 1.5\text{--}3.3$ μs), the periphery of the sheet is shifted vertically, e.g., into the region $y > 0$, then ($t \approx 3.5\text{--}4$ μs) the sheet moves to the region $y < 0$, i.e., reorientation of the current sheet takes place. When B_Z^0 is reversed, this situation is also reversed: the sheet moves from the region $y < 0$ to the region $y > 0$. In other words, during the evolution of the current sheet, its peripheral regions experience oppositely directed deviations from its midplane ($y = 0$).

Since the direction of B_Z^0 remains constant throughout the entire evolution of the current sheet, the observed reorientation of the sheet at the later stages indicates that Hall currents change direction. It was shown in [34] that the change of direction of Hall

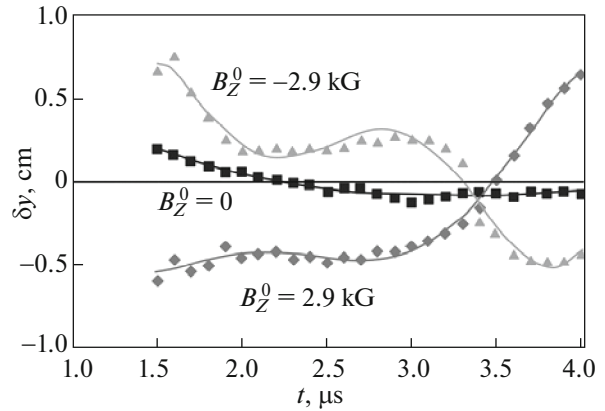


Fig. 11. Time dependence of the deviation of the maximums of current density δy from the midplane of the current sheet ($y = 0$) at $B_Z^0 = 0$; +2.9; -2.9 kG. Experimental conditions: $h = 0.5$ kG/cm, Ar, $p = 28$ mTorr.

currents occurs in the regions of the current sheet in which currents j_z appear that are directed oppositely to the main current in the central region of the sheet. The generation of reverse currents in current sheets and the consequences of their appearance are discussed in [16, 23, 26, 34–36].

Thus, Hall currents have a significant effect on the structure of current sheets that form in 3D magnetic configurations with X line and a longitudinal magnetic field component, and the shift of the peripheral regions of the sheet that appears due to the oppositely directed Hall currents is a part of dynamic processes in current sheets.

7. RELATION BETWEEN THE LONGITUDINAL COMPONENT AND TRANSVERSE GRADIENT OF MAGNETIC FIELD IN 3D MAGNETIC CONFIGURATIONS WITH X LINE AT WHICH FORMATION OF CURRENT SHEETS IS POSSIBLE

One of important tasks of studying the structure of current sheets that develop in 3D magnetic configurations with X line (1) is the determination of the range of initial conditions under which current sheets can be formed. Of particular interest is the maximum value of the longitudinal component B_Z^0 in the presence of which the current sheets can still develop, at a given value of the transverse magnetic field gradient h .

Analysis of the images of radiating plasma and results of magnetic measurements showed that the formation of current sheets can occur under conditions when the value of the B_Z^0 component exceeds the value of the transverse magnetic field in the majority or even in the entire plasma volume, $|B_Z^0| \geq |\mathbf{B}_\perp| = h \times |\mathbf{r}|$, at $|\mathbf{r}| \leq R_C$ (where R_C is radius of the vacuum chamber) [6,

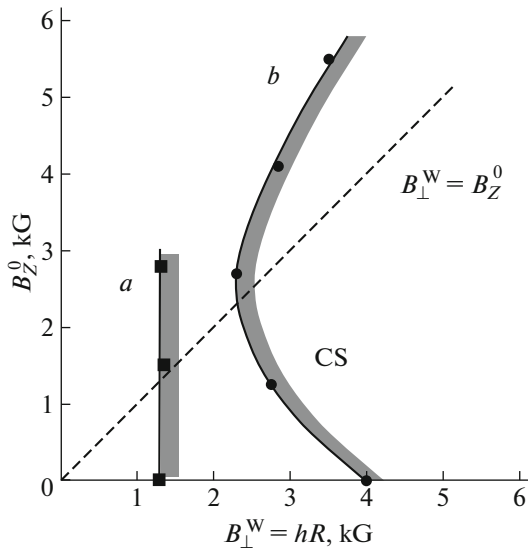


Fig. 12. Parameters of 3D magnetic configurations with X line in which the current sheets are formed. \mathbf{B}_\perp^W is transverse magnetic field at the plasma boundary and B_z^0 is the longitudinal magnetic field component. Experimental conditions: $J_z = 50$ kA, He, (a) $p_0 = 60$ mTorr, and (b) $p_0 = 300$ mTorr.

7, 9]. At the same time, the ratio B_z^0/h should not exceed some critical value which, under experimental conditions in the CS-3D device, was ≈ 15 cm.

It is possible to draw (Fig. 12) the boundaries of the regions where formation of current sheets is possible (to the right of both lines a and b) and where the sheets do not form (to the left of the same lines) in the plane ($|B_z^0|, |\mathbf{B}_\perp^W| = h \times R_C$). The position of each boundary line depends on the exact experimental conditions such as the density of initial plasma, the ion mass, and the plasma current [7, 9].

From this, it follows that the formation of current sheets in 3D magnetic configurations with X line is possible in a relatively wide yet limited range of initial conditions. The most important parameter that determines the possibility of current sheet formation is the gradient of transverse magnetic field h , which has to exceed a certain critical value.

8. CONCLUSIONS

In this review, results are presented of experimental studies of the evolution and structure of current sheets that can form in three-dimensional (3D) magnetic configurations with X line in the presence of a relatively strong magnetic field component directed along the X line. Such studies attract special interest because magnetic configurations with X line are widely presented in nature and in installations for confinement and heating of hot plasma. The possibilities of forma-

tion of current sheet and their properties determine the specific features of the processes of magnetic reconnection and transformation of magnetic energy stored in the vicinity of the current sheet into the thermal and kinetic energy of plasma and into flows of accelerated particles and radiation.

Despite their outward similarity, current sheets formed in 3D and 2D magnetic configurations have substantial differences in a number of parameters. The formation of the current sheet in the 3D magnetic configuration with a longitudinal magnetic field component directed along the X line leads to the trapping of this component by plasma flows and, in the end, to the increase in this component within the current sheet compared to its values outside the sheet.

One of the results of this process consists in the appearance of current that maintains the increased longitudinal magnetic field and flows in the transverse plane with respect to the main current in the sheet. This leads to the current structure in the sheet becoming more complicated: it becomes three-dimensional and substantially different from the planar “ribbon” current characteristic of current sheets that develop in the 2D magnetic configurations with null line.

Comparison of current sheets that develop in configurations with X line at different values of the longitudinal magnetic field component and in its absence shows substantial differences both in the distributions of the main current in the sheet and in plasma density distributions. In a series of experiments, it was shown that the increase in the longitudinal component leads to the decrease in the efficiency of compression of electric current and plasma into the sheet. This is caused by the increase of the longitudinal magnetic field component in the sheet compared to its value outside of it, which results in changing the pressure balance due to the appearance of excess field in the sheet.

In the presence of the longitudinal magnetic field component directed along the X line, the peripheral regions of current sheets experience oppositely directed deviations from its midplane, so that the sheet becomes tilted and asymmetric. These deviations manifest in the spatial distributions of the current that flows in the sheet and the plasma concentrated in the sheet. The deviations are maximum at the early stage of the sheet evolution and decrease in time, while the sign of the deviations reverses when the direction of the longitudinal component is reversed. It was shown that the discovered asymmetry of current sheets appears due to the excitation of Hall currents and arising additional dynamic effects under interaction of Hall currents with the longitudinal magnetic field component. In this, a satisfactory correlation was observed between the current density and plasma density distributions in asymmetric current sheets. It follows that Hall currents have a substantial influence on the structure of current sheets that form in 3D mag-

netic configurations with X line and a longitudinal magnetic field component.

It was shown that the formation of current sheets in 3D magnetic configurations with X line is possible in a relatively wide, but limited range of initial conditions and that the most significant parameter that determines the possibility of current sheet formation is the gradient h of transverse magnetic field, which has to exceed a certain critical value.

ACKNOWLEDGMENTS

To conclude, the author would like to express her gratitude to S.A. Savinov for useful discussions and his help in preparing this article for publication.

CONFLICT OF INTEREST

The author declares no conflict of interest.

REFERENCES

1. S. I. Syrovatskii, *Annu. Rev. Astron. Astrophys.* **19**, 163 (1981).
2. D. Biscamp, *Magnetic Reconnection in Plasmas* (Cambridge Univ. Press, Cambridge, 2005).
3. E. R. Priest and T. Forbes, *Magnetic Reconnection* (Cambridge Univ. Press, Cambridge, 2000).
4. B. B. Kadomtsev, *Rep. Prog. Phys.* **50**, 115 (1987).
5. A. G. Frank, *Plasma Phys. Control. Fusion.* **41**, A687 (1999).
6. S. Y. Bogdanov, N. P. Kyrie, V. S. Markov, and A. G. Frank, *JETP Lett.* **71**, 53 (2000).
7. A. G. Frank and S. Yu. Bogdanov, *Earth, Planets Space* **53**, 531 (2001).
8. S. Yu. Bogdanov, V. S. Markov, A. G. Frank, G. V. Dreiden, I. I. Komissarova, G. V. Ostrovskaya, and E. N. Shedova, *Plasma Phys. Rep.* **28**, 549 (2002).
9. A. G. Frank, S. Yu. Bogdanov, N. P. Kyrie, and V. S. Markov, *AIP Conf. Proc.* **703**, 431 (2004).
10. A. G. Frank, S. Yu. Bogdanov, V. S. Markov, G. V. Dreiden, and G. V. Ostrovskaya, *Phys. Plasmas* **12**, 052316 (2005).
11. S. Yu. Bogdanov, V. B. Buriлина, and A. G. Frank, *J. Exp. Theor. Phys.* **87**, 655 (1998).
12. A. G. Frank, *Phys.—Usp.* **53**, 941 (2010).
13. S. Yu. Bogdanov, S. G. Bugrov, V. P. Gritsyna, O. V. Zverev, G. V. Karpov, V. S. Markov, D. V. Repin, and A. G. Frank, *Plasma Phys. Rep.* **33**, 435 (2007).
14. A. G. Frank, S. G. Bugrov, and V. S. Markov, *Phys. Plasmas* **15**, 092102 (2008).
15. A. G. Frank, S. G. Bugrov, and V. S. Markov, *Phys. Lett. A* **373**, 1460 (2009).
16. A. G. Frank and S. N. Satunin, *Plasma Phys. Rep.* **37**, 829 (2011).
17. A. G. Frank and S. N. Satunin, *JETP Lett.* **100**, 75 (2014).
18. S. Yu. Bogdanov, G. V. Dreiden, V. S. Markov, G. V. Ostrovskaya, and A. G. Frank, *Plasma Phys. Rep.* **32**, 1034 (2006).
19. A. G. Frank, S. Yu. Bogdanov, G. V. Dreiden, V. S. Markov, and G. V. Ostrovskaya, *Phys. Lett. A* **348**, 318 (2006).
20. S. Yu. Bogdanov, G. V. Dreiden, N. P. Kyrie, V. S. Markov, G. V. Ostrovskaya, and A. G. Frank, *Plasma Phys. Rep.* **33**, 930 (2007).
21. G. V. Ostrovskaya and A. G. Frank, *Plasma Phys. Rep.* **40**, 21 (2014).
22. G. S. Voronov, N. P. Kyrie, V. S. Markov, G. V. Ostrovskaya, and A. G. Frank, *Plasma Phys. Rep.* **34**, 999 (2008).
23. A. G. Frank, N. P. Kyrie, and S. N. Satunin, *Phys. Plasmas* **18**, 111209 (2011).
24. N. P. Kyrie, V. S. Markov, A. G. Frank, D. G. Vasilkov, and E. V. Voronova, *Plasma Phys. Rep.* **42**, 549 (2016).
25. S. I. Syrovatskii, A. G. Frank, and A. Z. Khodzhaev, *JETP Lett.* **15**, 94 (1972).
26. A. G. Frank and S. N. Satunin, *Plasma Phys. Rep.* **44**, 190 (2018).
27. S. Yu. Bogdanov, G. V. Dreiden, N. P. Kyrie, I. I. Komissarova, V. S. Markov, G. V. Ostrovskaya, Yu. I. Ostrovskii, V. N. Philippov, A. G. Frank, A. Z. Khodzhaev, and E. N. Shedova, *Sov. J. Plasma Phys.* **18**, 654 (1992).
28. S. Yu. Bogdanov, Yu. F. Bondar, V. B. Buriлина, N. P. Kyrie, V. S. Markov, G. P. Mkhedize, A. A. Savin, and A. G. Frank, *Tech. Phys.* **39**, 877 (1994).
29. A. G. Frank, S. Yu. Bogdanov, V. B. Buriлина, N. P. Kyrie, and V. S. Markov, *Contrib. Plasma Phys.* **40**, 106 (2000).
30. A. G. Frank, A. V. Artemyev, and L. M. Zelenyi, *J. Exp. Theor. Phys.* **123**, 699 (2016).
31. A. G. Frank, G. V. Ostrovskaya, E. V. Yushkov, A. V. Artemyev, and S. N. Satunin, *Cosmic Res.* **55**, 46 (2017).
32. E. V. Yushkov, A. G. Frank, A. V. Artemyev, A. A. Petrukovich, and R. Nakamura, *Plasma Phys. Rep.* **44**, 1126 (2018).
33. A. G. Frank and S. N. Satunin, *Bull. Lebedev Phys. Inst.* **47**, 54 (2020).
34. A. G. Frank and S. N. Satunin, *JETP Lett.* **112**, 623 (2020).
35. A. G. Frank, N. P. Kyrie, S. N. Satunin, and S. A. Savinov, *Universe* **7**, 400 (2021).
36. A. G. Frank and S. N. Satunin, *Plasma Phys. Rep.* **48**, 10 (2022).

Translated by E. Voronova